Scientific Research Publishing

Journal of Building Construction and Planning Research, 2025, 13(2), 55-77
https://www.scirp.org/journal/jbcpr
ISSN Online: 2328-4897
ISSN Print: 2328-4889

Flexural and Shear Performance of RC Beam Strengthened with Different FRP Layers

Bashir H. Osman[1], Abu-Bakre A. Elamin[2]

[1]Civil Engineering Department, College of Engineering, University of Sinnar, Sennar, Sudan
[2]Civil Engineering Department, College of Engineering, University of Technology, Khartoum, Sudan
Email: bashir00@yahoo.com, abubakre55@yahoo.com

How to cite this paper: Osman, B.H. and Elamin, A.-B.A. (2025) Flexural and Shear Performance of RC Beam Strengthened with Different FRP Layers. *Journal of Building Construction and Planning Research*, **13**, 55-77.
https://doi.org/10.4236/jbcpr.2025.132003

Received: March 26, 2025
Accepted: June 17, 2025
Published: June 20, 2025

Abstract

This paper presents numerical research on carrying capacity of reinforced concrete (RC) beams strengthened by external flexural and flexural-shear carbon fiber reinforced polymer (CFRP). First the model is verified with previous published work to ensure that the results obtained from FE by using ANSYS are correct, the results were in accordance with those from published experiments with variation not more than 20%. The FRP layers and thickness were considered as main parameters. Furthermore, the work carried out examined both the flexural and flexural-shear strengthening capacities of retrofitted RC beams and indicated how different strengthening arrangements of CFRP sheets affect the mechanical behavior of the strengthened RC beams. Moreover, the stiffness, ultimate strength and hardening behavior of the RC beam for different strengthening schemes are investigated by the established finite element model. The results show that the FRP layer and thickness have greater effect for increasing the load caring capacity of beams with increasing of 60%, 40%, and 30% for three, two, and one layer, respectively, compared with those without strengthening.

Keywords

RC Beam, Flexural-Shear, ANSYS, CFRP, FE Analysis

1. Introduction

Reinforced concrete (RC) beams are essential structural components in buildings, bridges, and other infrastructures. Over time, these beams may experience deterioration or a reduction in their load-carrying capacity due to factors such as aging, corrosion of reinforcement, overloading, or environmental exposure. In many cases, the need for strengthening arises to ensure the safety and longevity of the structure without the need for costly and disruptive replacement. One of the most innovative and effective methods for strengthening reinforced concrete beams is the use of Fiber Reinforced Polymers (FRP). Different bonding techniques have insignificant effects on shear strengthening but have a positive impact on flexural strengthening [1] [2]. FRP composites are advanced materials made by combining high-strength fibers, such as carbon, glass, or aramid, with a polymer resin. This composite material is known for its excellent strength-to-weight ratio, corrosion resistance, and versatility [3]. When applied to RC beams, FRP can enhance structural performance, providing a significant increase in strength, stiffness, and durability [4] [5]. The FRP strengthening technique involves bonding the composite material to the tension or compression faces of the beam, depending on the failure mode and the desired outcome. This solution offers a non-invasive and relatively easy-to-apply method for improving the structural capacity of concrete beams without the need for extensive modifications. Furthermore, the lightweight nature of FRP materials reduces the overall weight of the structure, making it ideal for retrofitting existing infrastructure without adding significant additional load [6] [7].

This method of strengthening has gained widespread acceptance in the civil engineering industry due to its high efficiency, cost-effectiveness, and ability to provide long-lasting solutions for strengthening reinforced concrete beams. The use of FRP composites also ensures minimal disruption to the structure's operation, making it an attractive alternative for upgrading aging infrastructure or increasing the load-bearing capacity to meet modern demands. In this context, FRP strengthening is revolutionizing the way engineers approach structural rehabilitation and retrofitting, offering both immediate and long-term benefits for reinforced concrete beams investigated four specimens to study the shear strengthening of deficient reinforced concrete (RC) beams using carbon fibre-reinforced polymer (CFRP) sheets [8]-[15]. The effect of the pattern and orientation of the strengthening fabric on the shear capacity of the strengthened beams were examined and his result obtained that the ultimate failure of strengthened beams occurred with delayed cracking of concrete eventually leading to the rupture of CFRP sheets and pulling of concrete on side and/or side cover delamination depending on the strengthening patterns.

The potential of using carbon fiber reinforced Polymer (CFRP) as reinforcement to concrete Beam was investigated by Norazman Mohamad Nor, *et al.* (2013) [16]. The CFRP reinforcement is applied in strip form, which is more economical compared to wrapping or forming it into bar shape, because it is easier and uses less fiber to achieve similar performance. Furthermore, CFRP reinforced concrete beam gives the required resistance and strength as designed, with behavior more advantage than those reinforced with steel bars [17]-[19]. The understanding of the shear resisting mechanisms in RC beams shear-strengthened by externally bonded fiber-reinforced polymer (FRP) sheets was illustrated by Denise Ferreira, *et al.* (2013) [20]. They analyzed and studied the effects of the contribution of FRP ratio on concrete, transversal steel strains and stresses, longitudinal tensile steel stresses, and diagonal compression struts and numerical results were compared with eight existing experimental results and the influence of the FRP sheets on the shear strength of the beam. They concluded that the presence of FRP reinforcement modifies the inclinations of cracks and struts, and other parameters related to the shear response, producing great effects on the shear strength of the RC beams. FRP strengthening reinforced concrete beams using Finite element (FE) studies were performed and carried out in many studies [21]-[24]. The numerical models able to predict the responses of FRP shear strengthened elements in an accurate and simple manner are needed for a wider and more efficient application of this measure in practice. Other studies have been carried out to investigate the flexural and shear behavior of bolted side-plated beams and coupling beams as well as the behavior of the connecting bolt groups [22]. In this paper, RC beams strengthened with FRP are simulated firstly by using finite element software ANSYS for validation. And then the results from FEM will be calibrated with published experimental data to ensure that the simulation process is correct. The effect of FRP thickness on RC beam capacity is studied.

2. Research Program

The research program includes two parts; the first part is the validation of the proposed FE model using published experimental tests and the second part is concerned with parametric study. This study investigated the effects of the different FRP layers on the strength of RC beams. The published experimental results were compared with those obtained from FE method to provide background knowledge for establishing modeling rules, and more confidence for RC beams strengthened with FRP by using software. The findings of the present study will also guide further studies in the field. Materials properties which published in Roaa Babiker 2024 [18] was used to model the beam in ANSYS finite element program.

2.1. Finite Element Modelling (FEM)

The materials properties of modeled beams are shown in **Figure 1**. Due to the symmetry of geometry, loading, boundary conditions, and material properties, a quarter FE model was built and analyzed. The use of a quarter model significantly reduces computational time. In ANSYS terminology, the term model generation usually takes on the narrower meaning of generating the nodes and elements that represent the spatial volume and connectivity of the actual system [25].

Thus, model generation in this discussion will mean the process of defining the geometric configuration of the model's nodes and elements. From the available element library in ANSYS, the elements used in this work as fallow:

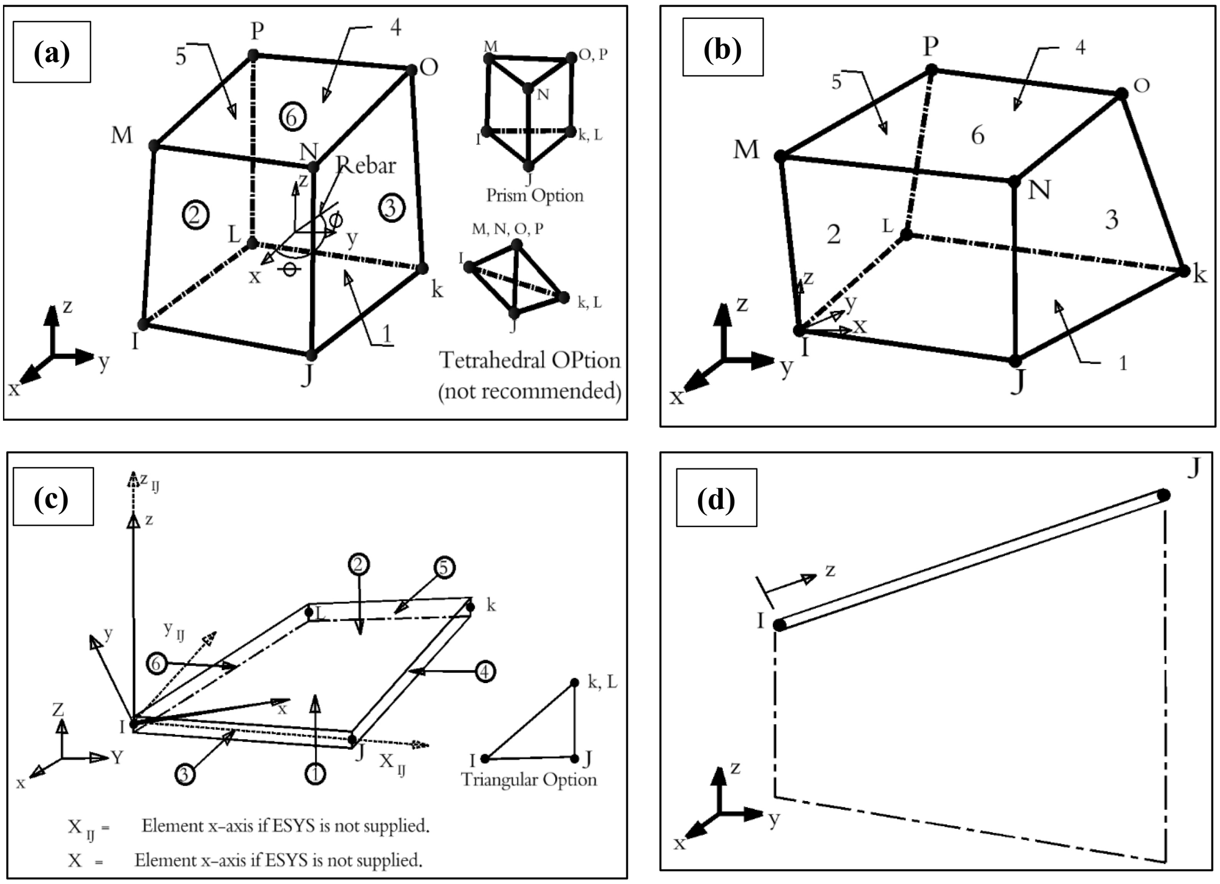

Figure 1. (a) Solid65—3-D reinforced concrete solid; (b): Solid45—3-D solid; (c) Shell 181-FRP; (d) LINK8-for steel reinforcement (ANSYS 14.5).

2.1.1. Reinforced Concrete

An eight-node solid element, Solid65, was used to model the concrete. The solid element has eight nodes with three degrees of freedom at each node –translations in the nodal x, y, and z directions. The element is capable of plastic deformation, cracking in three orthogonal directions, and crushing. The value of the shear transfer coefficient (βt) ranges from 0.0 to 1.0, with 0.0 representing a smooth crack and 1.0 representing a rough crack. In this paper, a shear transfer coefficient of the open crack of βt is 0.25, and a shear transfer coefficient of closed crack βc is 0.8 are used. The modulus of elasticity (E_c), and the modulus of rupture (f_r) for concrete both are calculated in terms of the concrete compressive strength ($f_c^{/}$)

$$E_c = 4700\sqrt{f_c^{/}} \tag{1}$$

$$f_r = 0.62\sqrt{f_c^{/}} \tag{2}$$

The Poisson's ratio for concrete is usually taken as 0.2 and the stress strain relationship can be obtained from following equations.

$$f = E_c\varepsilon \Big/ \left(1 + \left(\varepsilon/\varepsilon_0\right)^2\right) \tag{3}$$

$$\varepsilon_0 = \frac{2 f_c^{/}}{E_c} \tag{4}$$

$$E_c = \frac{f}{\varepsilon} \tag{5}$$

Where f strees at any strain (ε), ε is strain at stress (f), ε_0: strain at the ultimate compressive strength $f_c^{/}$.

2.1.2. Reinforced Steel

nk-8 element was used to model steel reinforcement. Two nodes are required for this element. Each node has three degrees of freedom, – translations in the nodal x, y, and z directions. The element is also capable of plastic deformation. The geometry and node locations for this element type.

2.1.3. Steel Plates

An eight-node solid element, Solid45, was used for the steel plates at the supports in the beam models. The element is defined with eight nodes having three degrees of freedom at each node – translations in the nodal x, y, and z directions.

2.2. Strengthening Model Technique

To study the contact between two bodies, the surface of one body is conventionally taken as a contact surface and the surface of the other body as a target surface. ARGE170 is used to represent various 3D target surfaces for the associated contact elements (CONTA175). CONTA175 may be used to represent contact and sliding between two surfaces (or between a node and a surface, or between a line and a surface) in 2D or 3D. The element is applicable to 2D or 3D structural contact analyses. Here in this study, concrete is considered as contact and the FRP as target element [24]. For concrete, ANSYS computer program requires input data for material properties such as Mishing, materials contact and target, boundary condition and the uniaxial stress-strain relationship for concrete in compression.

3. Verification Study

The FE model was calibrated with the published experimental study. The specimens tested by Roaa Babiker 2024 [18] shown in **Figure 2(a)** were modeled in the FE simulation.

3.1. FE Failure Criteria

For a FE model of RC beams, failure was considered when a solution for a 10 N load increment could not reach a convergence. The FE models of the beams typically failed when shear steel reinforcement yielded followed by severe cracking of concrete. This in turn caused the FE simulation to terminate due to a divergence. Divergence in the FE solution coincided with a considerably large deflection, exceeding the displacement limitation of the ANSYS software.

3.2. Model Description

Four reinforced concrete beams were tested, one beam without strengthening and considered as reference beam, one beam was strengthened with FRP without pre-damage and two other beams were strengthened after subjected to pre-damage load. Each beam possessed a rectangular section with dimensions of 1200 mm × 100 mm × 200 mm. The beams were reinforced with stirrups of 6-mm diameter spaced 120-mm center to center. The longitudinal tensile reinforcement with a diameter of 10 mm was provided in the top and bottom of the beam.

When the beam BM1 was considered as control beam without strengthening, BM2 and BM3 were exposed to an elastic load by cracking up to 50% and 75% of the control beam's load capacity, respectively, before being strengthened with CFRP. BM4 was strengthened and tested to failure load without pre-loading.

The goal of the comparison between the FE model by using ANSYS14.5 and the experimental results was to ensure that the material properties, elements, and convergence criteria are adequate to model the response of the member and make sure that the simulation process is correct. Therefore, in this study, the beams which conducted in the previous experimental test were simulated for verification study. Figure 2 shows the geometry and tested beams. The comparison between experimental and FE results by using ANSYS were illustrated in Figure 3. From Figure 3, it is evident that there was a good correlation between the numerical and experimental load-deflection curves at all loading stages. The FE models were able to predict accurately the load capacities for the simulated RC beams. This confirmed the validity of the developed FE models and reliability of the FE simulation. Table 1 showed the numerical and experimental cracking and failure loads for the calibrated beams.

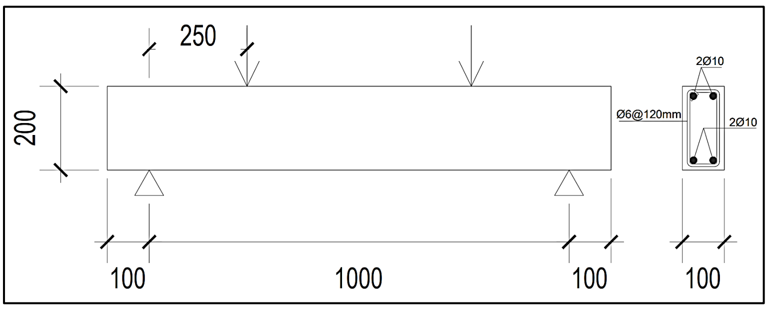

(a)

(b)

Figure 2. Tested beams (a) Geometry; (b) Failure modes beams.

As shown from Table 1 that the results obtained from FE analysis are in accordance with those from experimental works with variation of not more than 20%.

Table 1. FE and Experimental failure and cracking loads of tested beams.

Specimen	Cracking load (kN)		Exp./FE (cracking load) %	Failure load (kN)		Exp./FE (failure load) %
	Exp.	FE		Exp.	FE	
BM1	34.11	29	1.17	84.68	88	0.96
BM2	33.68	27	1.24	123.01	130	0.95
BM3	35.70	32	1.12	112.86	122	0.93
BM4	-	26	-	111.74	118	0.94

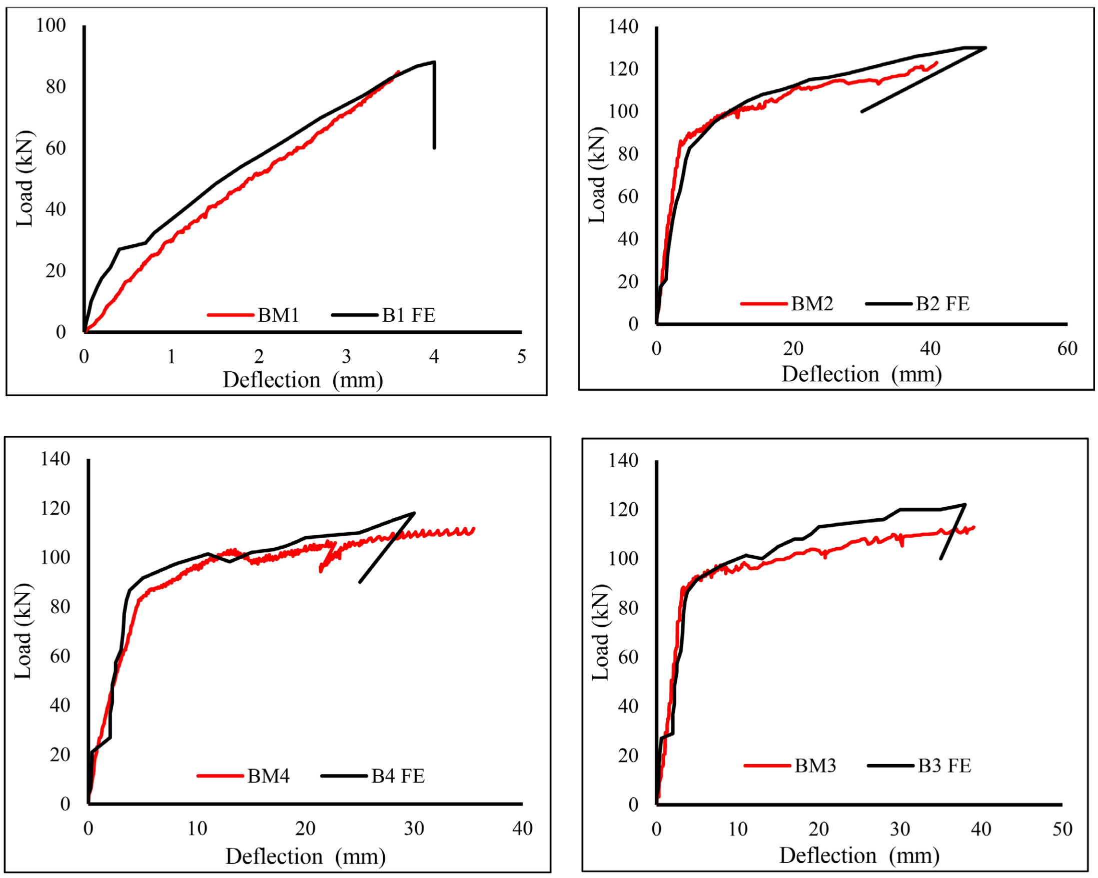

Figure 3. Load-deflection relationship for tested beams compared with FE results.

3.3. Modeling RC Beam Description

For parametric study, a rectangular reinforced concrete beam was conducted by using ANSYS finite element model. The model program includes instrumentation, and four RC beam specimens with 400 mm depth, 150 mm width, 2300 mm length and 2000 mm clear span. In these beam specimens, the same steel reinforcement layout was provided, where two tensile steel bars with 12-mm diameter were arranged to the bottom of beam, two tensile steel bars with 10-mm diameter were arranged to the top of beam, shear reinforcement spacing 200 mm with 8 mm diameter stirrups were used throughout the entire beam length. The thickness of the concrete cover layer was 25 mm at the lateral and upper faces of the beam and 35 mm at the bottom side which have 360 Mpa yield strength for basic iron and 240 Mpa for links. The dimensions and details of the modeling beams are presented in Figure 4. The used CFRP strips have a width of 150 mm and a thickness of 1.1 mm per layer.

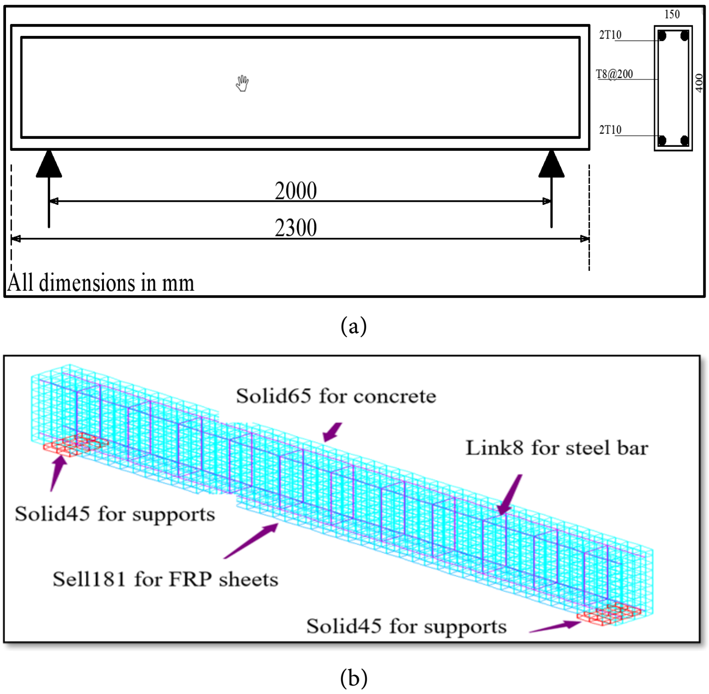

Figure 4. Studied beam (a) Layout geometry; (b) FE model.

4. Parametric Study on Flexural Shear Performance for RC Beam with Different FRP Layers

Based on the established finite element model in ANSYS software, the whole deformation and failure process are simulated for three type layouts of CFRP on the RC beam bottom. To explore the effect of these CFRP strengthen schemes on stiffness, ultimate carrying capacity of RC beam, the failure process of RC beam without CFRP is also modeled.

4.1. Results and Discussion

The obtained vertical displacement distributions of reinforced concrete beam for four different cases are presented in Figure 5, the maximum deflections are shown in Table 2. As shown from the results, deformation distribution features are almost same by comparing these subfigures, but the value of maximum deflection is very distinct. Especially, the maximum deflection decreases with the increase of CFRP layers. The Misses stress of reinforcing bars beam for three different cases are presented in Figure 6, where the maximum stress of reinforcing bars with different layers of FRP is presented in Table 3. The Misses stress and maximum stress distributions of FRP with different layers are presented in Figure 7 and Table 4, respectively. The horizontal stress distribution and evolution of concrete beam for four different cases are presented in Figure 8, Figure 9, Figure 10 and Figure 11, respectively. The results of the load-deflection curve are shown in Figure 12.

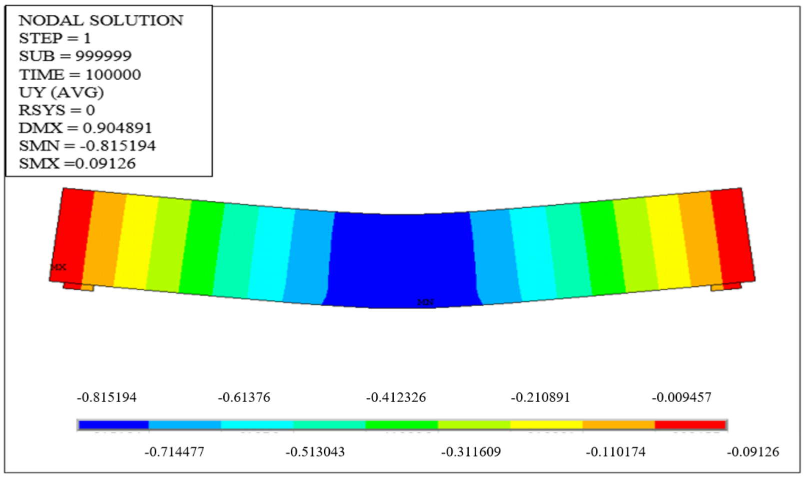

(a) Without-FRP

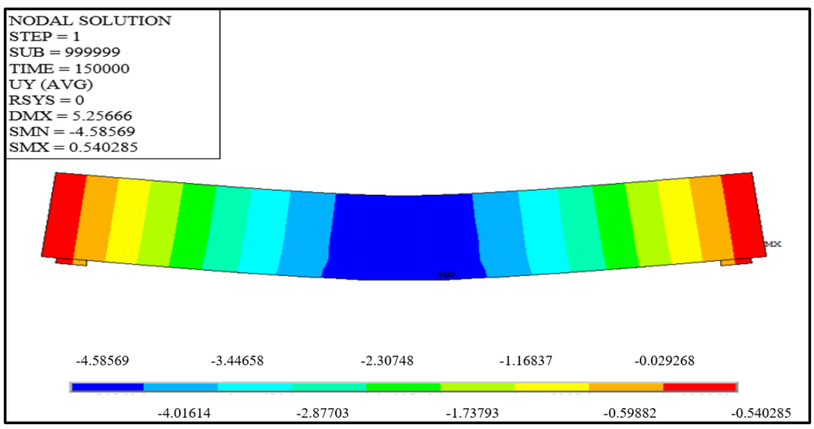

(b) One layer

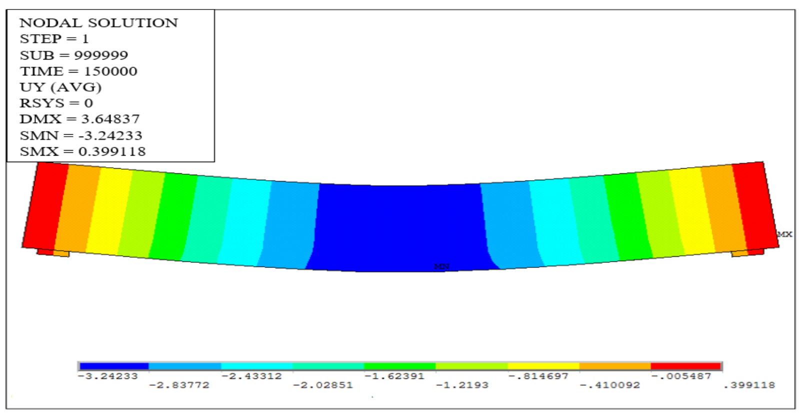

(c) Two layers

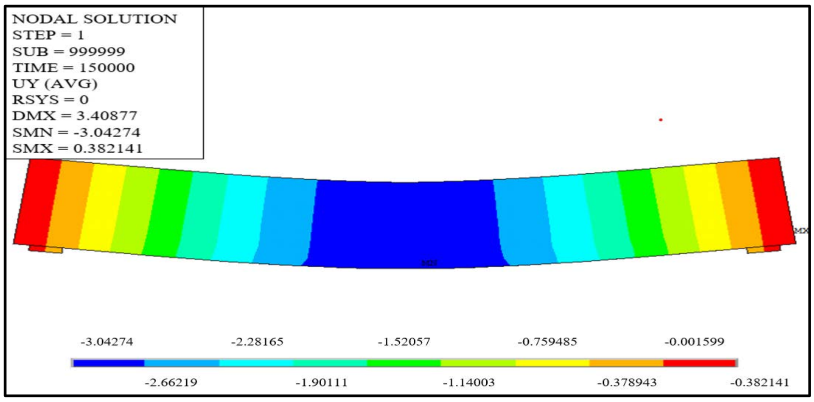

(d) Three layers

Figure 5. Vertical displacement values for reinforced concrete beams with different CFRP layers.

Table 2. Maximum deflection of RC beam with different layers of FRP.

Strengthening type	Without-FRP	One layer	Two layers	Three layers
Maximum Deflection (mm)	−0.815194	−4.58569	−3.24233	−3.04274

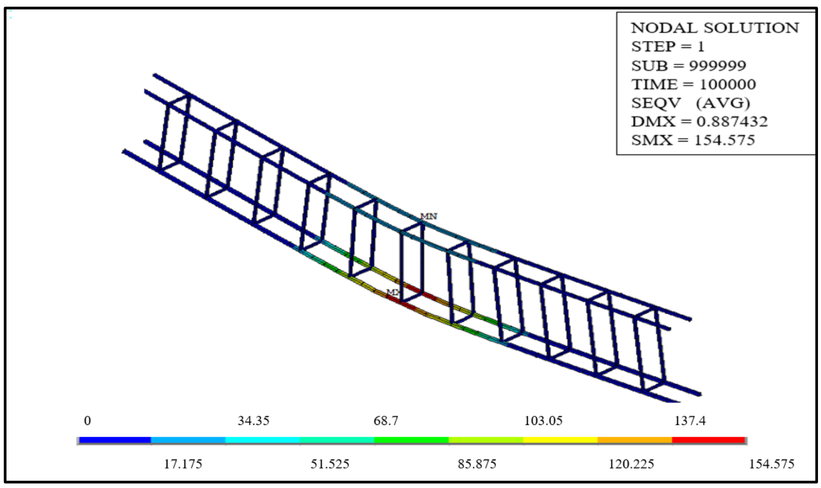

(a)

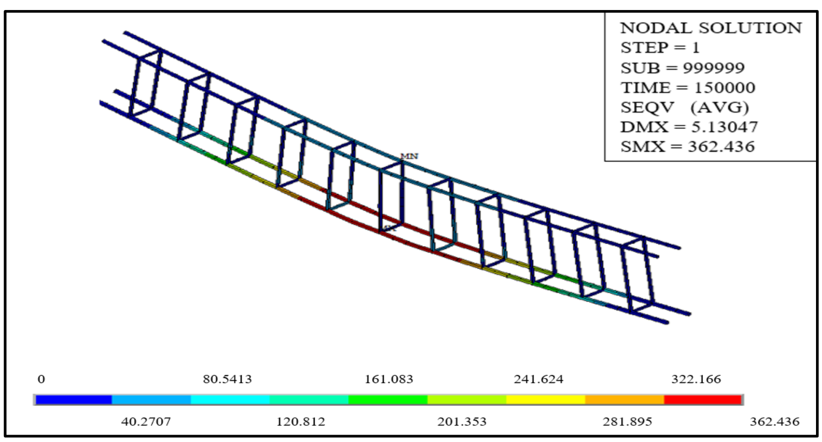

(b)

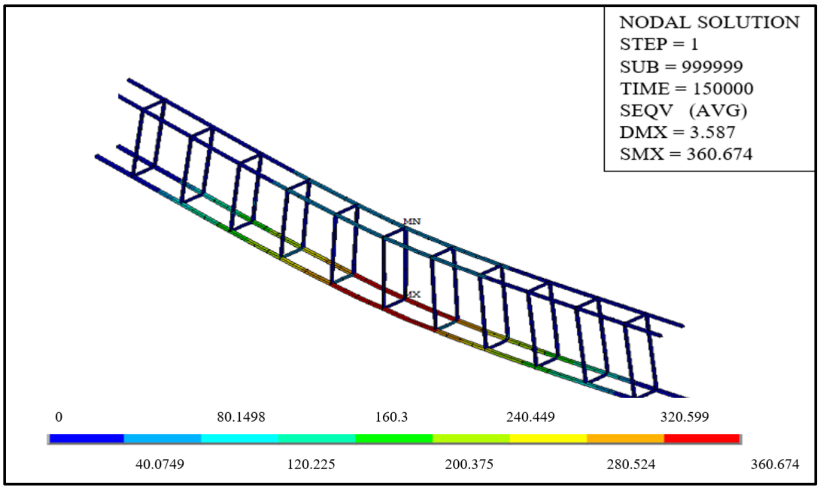

(c)

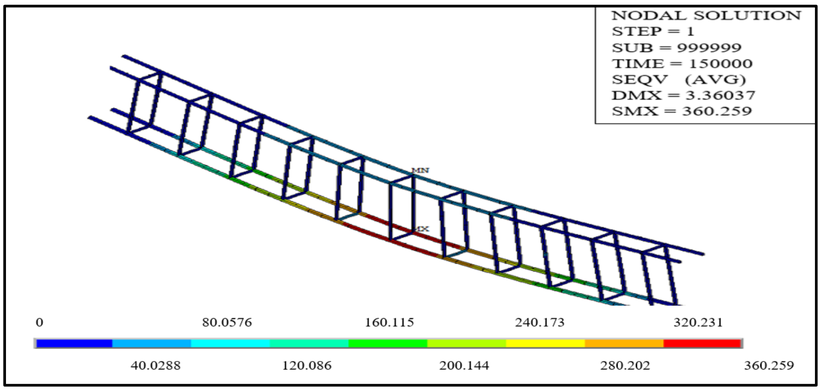

(d)

Figure 6. Misses Stress of the reinforcing bars (a) control; (b) one layer; (c) two layers; (d) three layers.

Table 3. Maximum stress of reinforcing bars with different FRP layers.

Strengthening type	Without-FRP	One layer	Two layers	Three layers
Maximum stress (MPa)	154.575	362.436	360.674	360.256

From Table 2, we find that the maximum deflection for the case of without FRP is the minimum, while the maximum deflection of other cases with FRP is much larger than that of the case without FRP. For comparison, the deflection increased in strengthened beams when the number of layers increased, which resulted in greater capacity compared with control beam. The deflection increased by 464%, 290%, and 260% for one, two, and three layers, respectively. This is because the brittle fracture happened easily in the non-strengthened beam, causing the RC beam without FRP strengthening fail earlier than the strengthened one. Furthermore, when reinforced using FRP at bottom side of the beam, the stiffness is improved especially for two layers case compared with one layer. However, the improvement effect is not obvious for three layers case. Therefore, from the point of deformation control, the optimized reinforcement scheme should be the two layers FRP case.

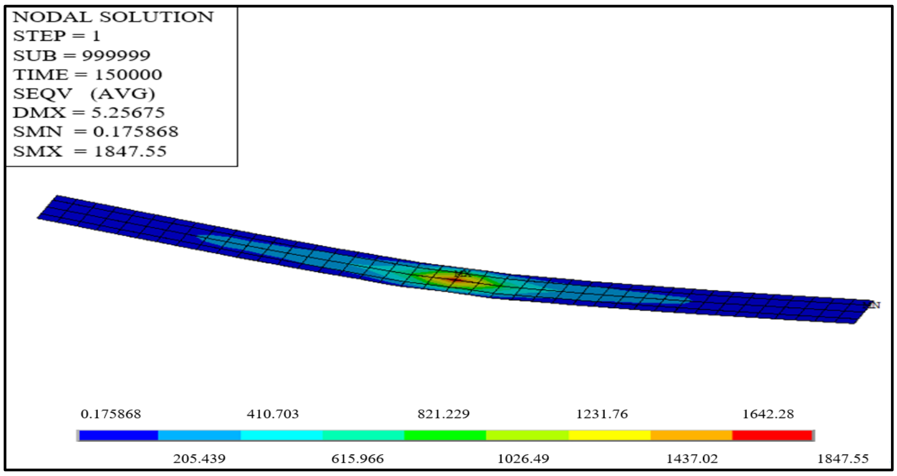

(a) One layer

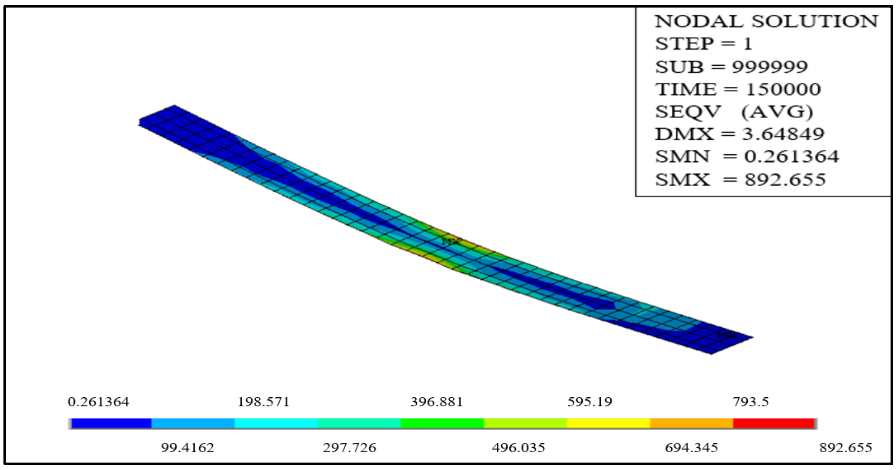

(b) Two layers

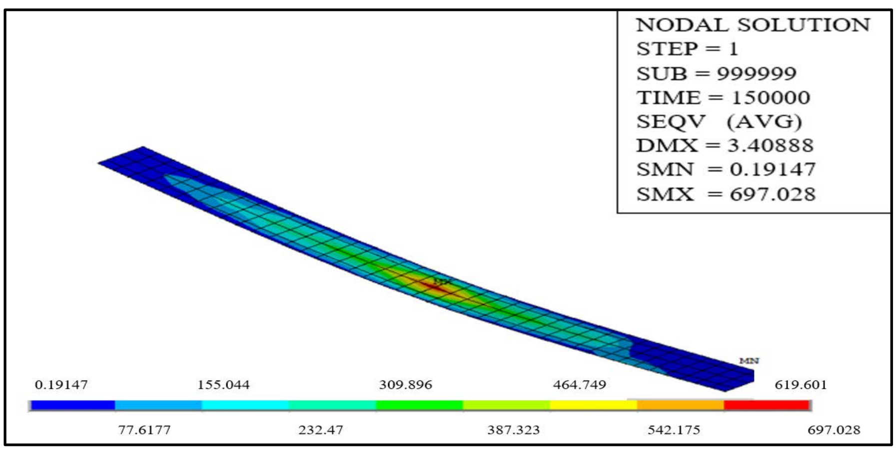

(c) Three layers

Figure 7. Misses Stress distribution of FRP.

From **Figure 6** and **Table 3**, the maximum stress in reinforcing bar for the case of without FRP is minimum, only 154.575 MPa, which is much less than that of the other cases with FRP. This due to the whole brittle fracturing happened earlier for the non-strengthened beam. In addition, when reinforced using FRP at bottom of RC beam, the carried part of external force for reinforcing bar is almost same for different layers of FRP due to most of the external force is passed on the CFRP at the bottom of RC beam. All the maximum stress in reinforcing bars happens in the middle of the beam span as shown in Figure 7 and Table 4.

Table 4. The maximum stress of FRP with different layers of FRP.

Strengthening type	Without-FRP	One layer	Two layers
Maximum stress (MPa)	1847.55	892.655	697.028

As shown from Figure 7 and Table 4, the maximum stress in one-layer FRP is 1847.55MPa, which is more than that of the two FRP layers. This is because most of the stress is carried by the first layer before the contribution of two layers start. Moreover, the maximum value of Misses stress also occurs at the center of the CFRP for all the four cases.

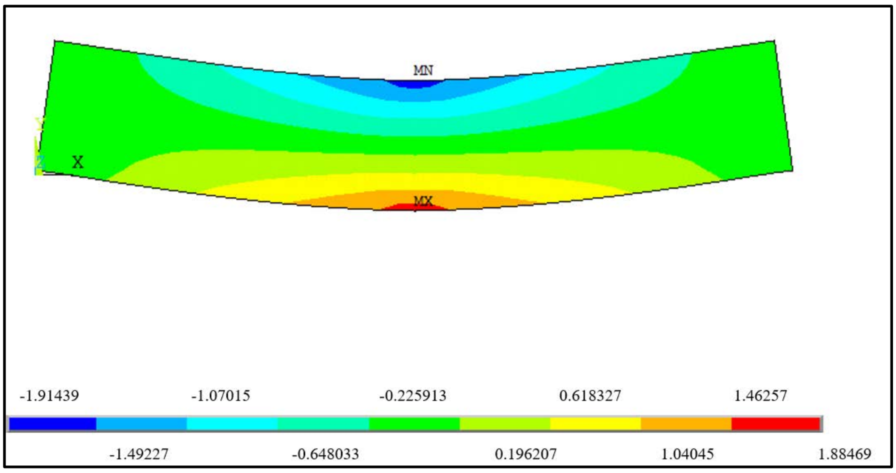

6th step

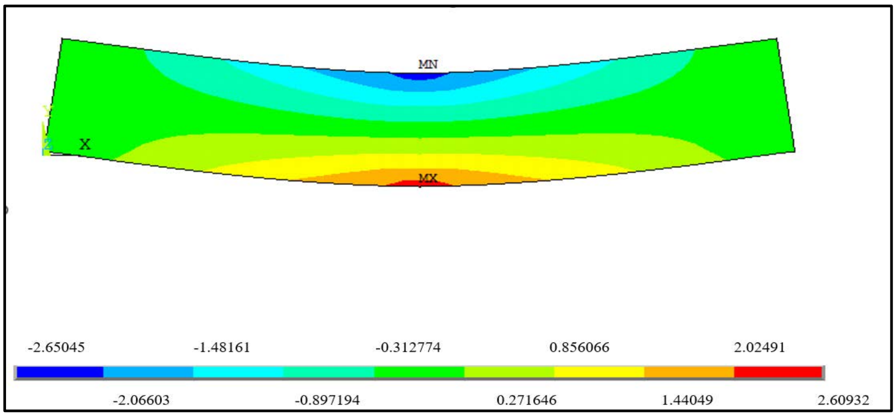

9th step

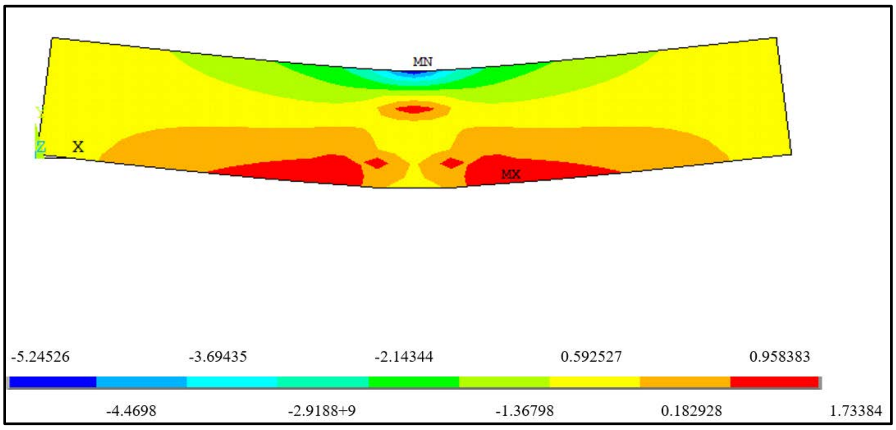

10th step

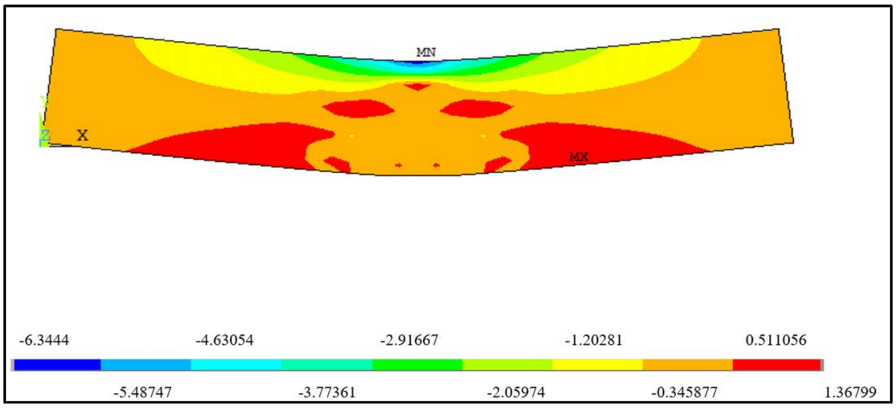

16th step

Figure 8. Different steps of stress distribution in x direction for the specimens without CFRP.

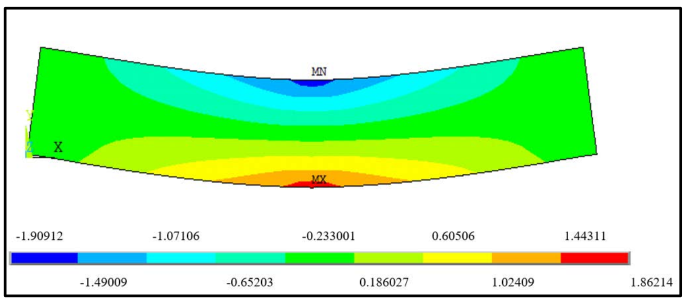

6th step

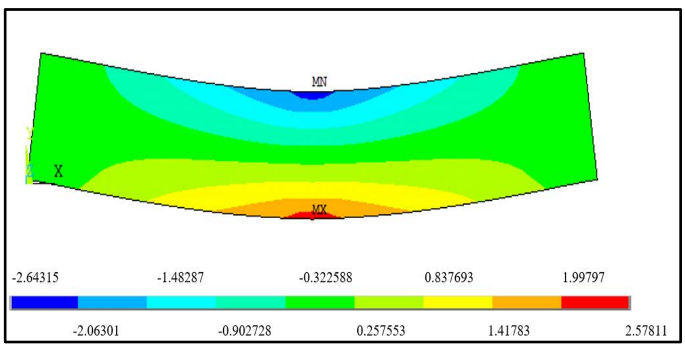

9th step

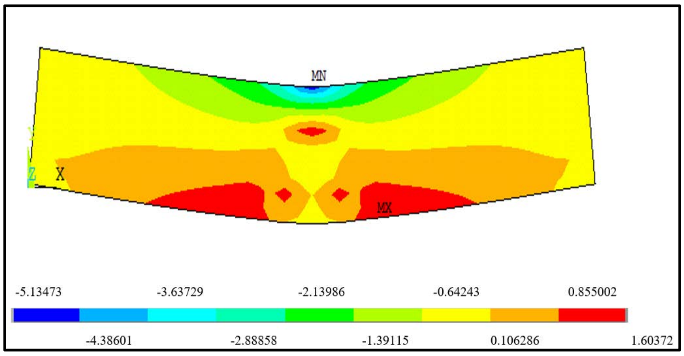

10th step

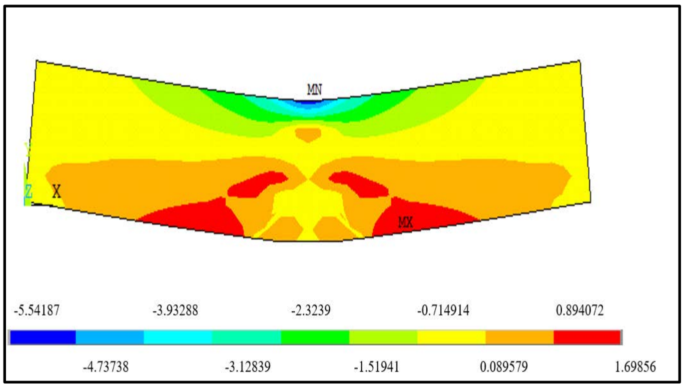

13th step

Figure 9. Different steps of stress distribution in x direction for specimens with one-layer CFRP.

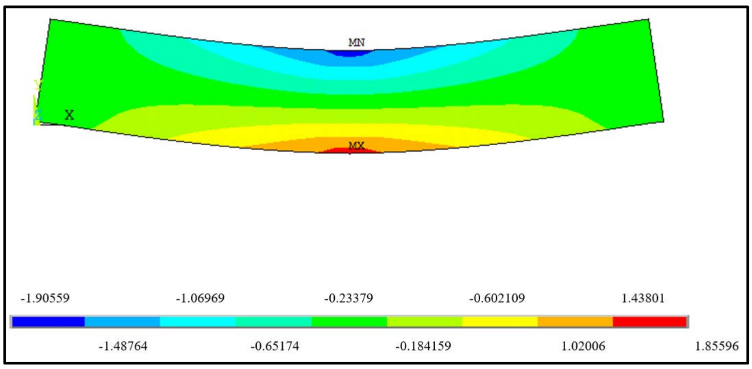

6th step

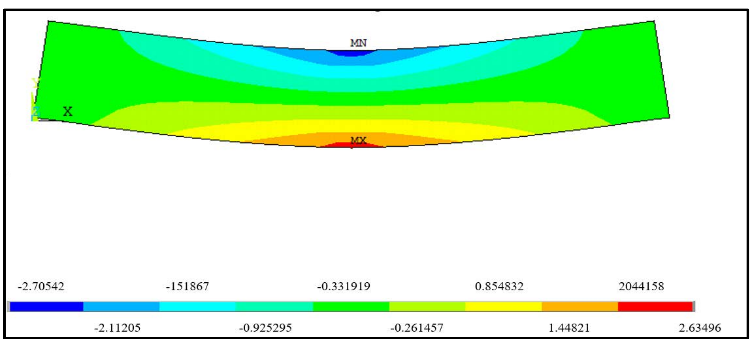

10th step

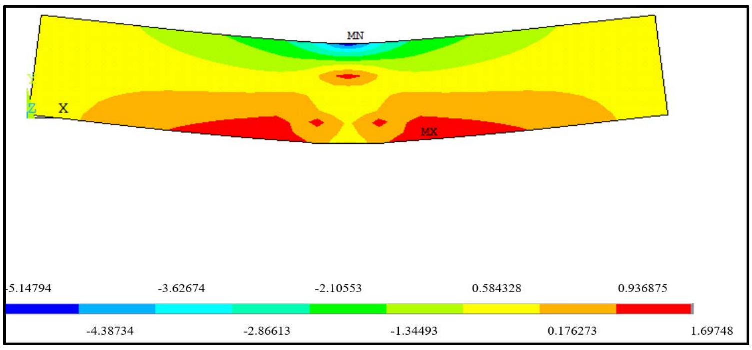

11th step

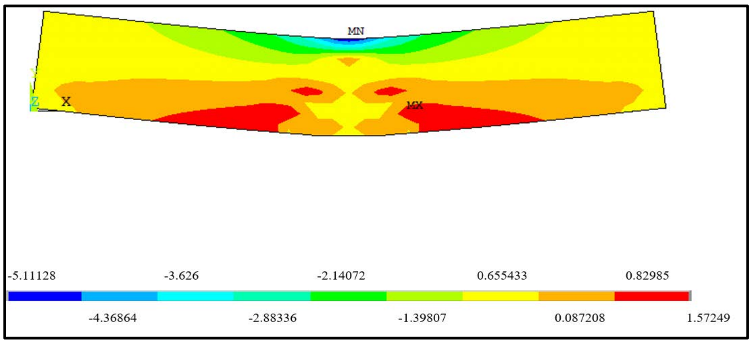

13th step

Figure 10. Different steps of stress distribution in x direction for specimens with two layers CFRP.

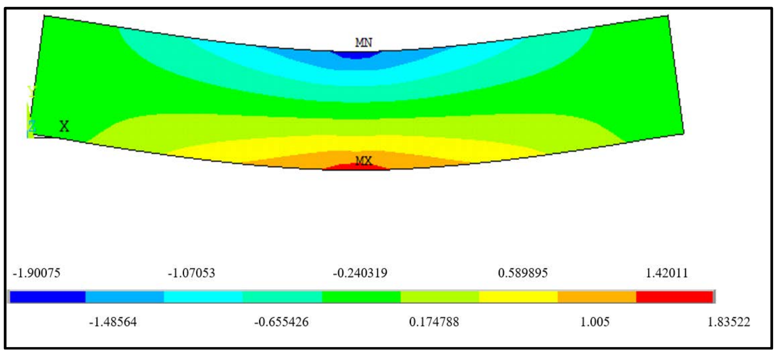

6th step

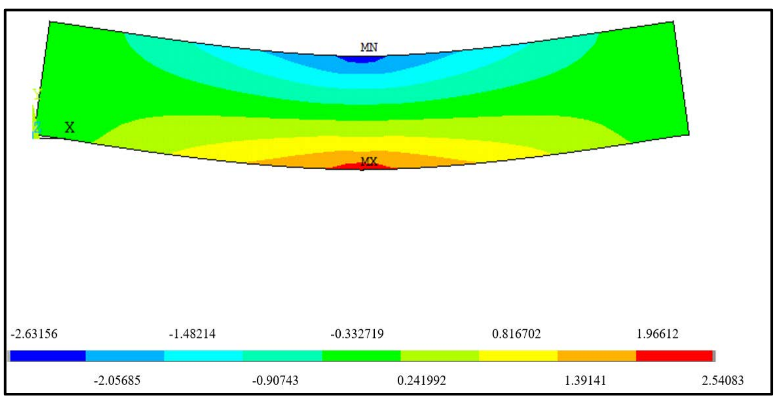

9th step

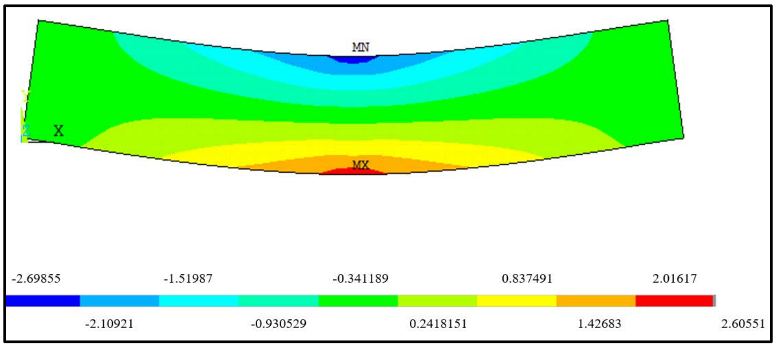

10th step

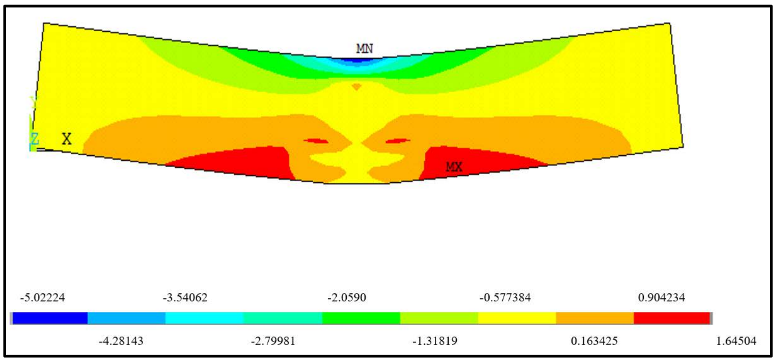

13th step

Figure 11. Different steps of stress distribution in x direction for specimens with three layers CFRP.

As shown from Figures 8-11, the tension stress is distributed at the bottom of beam, while the compression stress is distributed at the top of beam.

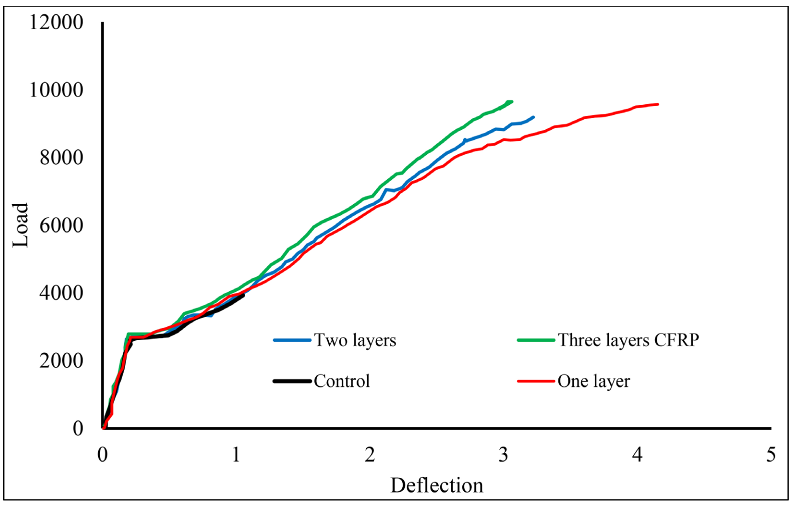

Figure 12. The load-deflection curves with different layout scheme of CFRP.

Once the maximum tension stress of middle span reaches the tensile strength of concrete material, the concrete beam will fracture along top direction from bottom at the middle span gradually, where the maximum tension stress is suddenly dropped while the compression stress at the top of beam is suddenly increased much more.

From the load-deflection curves shown as Figure 12, the results show that the FRP layer and thickness has greater effect for increasing the load caring capacity of beams with increasing of 60%, 40%, and 30% for three, two, and one layer, respectively, compared with those without strengthening. Accordingly, the deflection increases with an increase of load applied at mid span of the beam, while in the yield and fracturing stage of concrete it decreases with the increase of CFRP layer number. In the elastic stage, the deformation is almost the same for the different cases with and without CFRP. Once reaching the initial bearing capacity of RC beam, the plastic flow happens and holds for some seconds until the bearing capacity is regained due to the bearing action of CFRP.

4.2. The Fracturing Process of RC Beam without CFRP

By setting the failure parameters of concrete material, the generated cracks can be simulated. The parameters and coefficients used in FE simulation are: open shear transfer coefficient $\beta_t = 0.5$, the closed shear transfer coefficient $\beta_c = 0.9$, uniaxial cracking stress $f_t = 2.5MPa$, uniaxial crushing stress $f_c = 25MPa$ and biaxial crushing stress $f_b = 30MPa$. And when the hydrostatic pressure is $\sigma_m = 20MPa$, the hydro biaxial crushing stress $f'_b = 40MPa$, the hydro uniaxial crushing stress $f'_c = 35MPa$. The tensile crack factor $R^t = 0.5$. The fracturing results with the increase of load or time are as Figure 13.

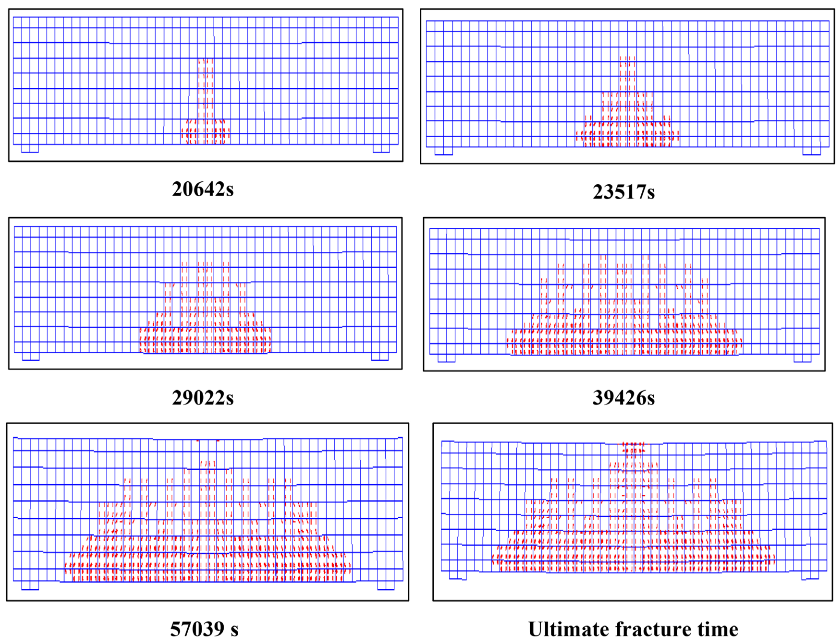

Figure 13. Generated cracks at different times (Second).

From crack distribution occurred, the cracks first happened in the middle of span and gradually developed along two sides. As load increases, the cracks number and width are increased and distributed along the bottom of the beams which lead to failure.

4.3. The Fracturing Process of RC Beam with One-Layer CFRP

The first crack at the integration points is as presented in Figure 14. From this figure, the first cracks developed from the bottom of mid-span diagonally to the top end, then gradually continued to the beam sides.

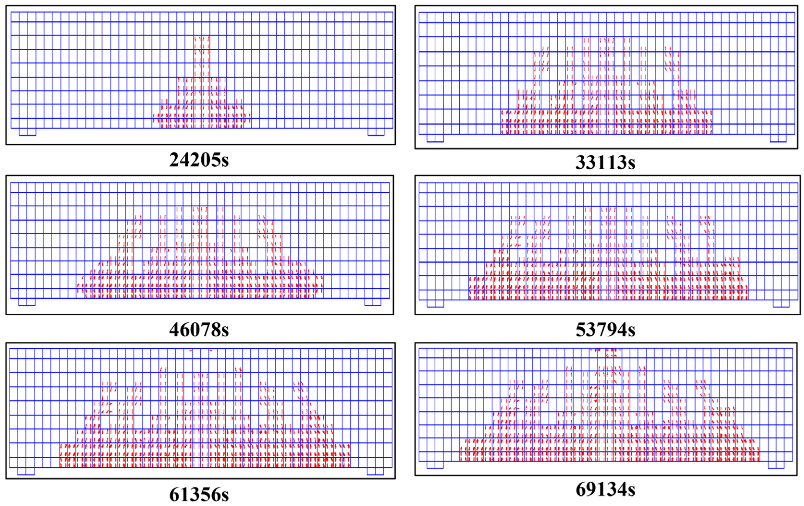

Figure 14. Generated cracks at different times one-layer CFRP (Second).

4.4. The Fracturing Process of RC Beam with Two Layers CFRP

The first cracks at integration points for beam strengthened with two layers FRP are presented in Figure 15.

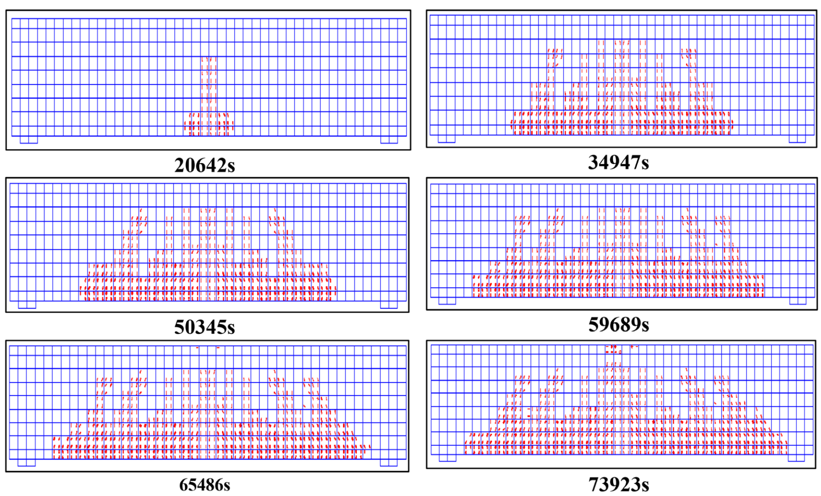

Figure 15. Generated cracks at different times two-layers CFRP (Second).

4.5. The Fracturing Process of RC Beam with Three Layers CFRP

The first cracks at integration points for beam strengthened with three layers FRP are presented in Figure 16.

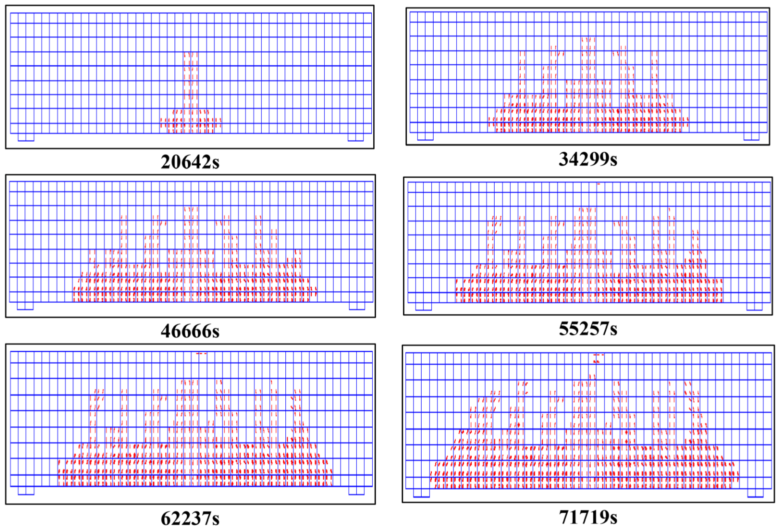

Figure 16. Generated cracks at different times three-layers CFRP (Second).

According to the results blotted in the above figures, the first cracks appeared at mid-span in all specimens and then propagated to other beam chords according to load increasing and strengthening. During the first loading steps, no cracks appeared at a small force, and the initial flexural cracks were distributed at a length of 15 mm right and left sides from beam loading point during step 20,142 s (20.142 kN) in specimens with one-layer CFRP. In addition, beams with two and three layers CFRP have the same crack width at initial load step 20,642 s. The maximum displacements of these beams in the initial steps donated were less than the yield displacements, which resulted in small cracks. Moreover, the beams that had been strengthened with CFRPs exhibited elastic behavior under applying loads. The entire beam failed due to the flexural of the longitudinally reinforcing. As shown from control beam, when the applied load increased, the crack had increased and covered about 85% of the spacemen length with corresponding load of 57.039 kN. However, the beams strengthened with two and three layers of CFRP show more crack distribution with high capacity compared with control beam, this due high contribution of CFRP. Furthermore, the beams with three layers of CFRP have greater capacity compared to other specimens, as shown in Figure 16 which the crack was covers about 92.5% of beam length with load step 62 kN prior to failure. In addition, this beam has failed at a load of 71.719 kN with crack distributed on 97.5 of beam sections. According to the measurements made during the simulation, the diagonal cracks in control beam, which was reinforced with ordinary steel, appeared at top of beam at load step 57.039 kN. In addition, the diagonal cracks appeared at top of beams strengthened with one, two and three layers of CFRP measured at load step 55.486 kN, 61.356 kN and 65.257 kN respectively. The crack damage of all the specimens at the end of the simulations occurred due to concrete cover spalled off and longitudinal reinforced steel was yielded and

CFRP was ruptured without debonding because it modeled contacted with concrete as full bond. In conclusion, the bearing capacity improved with the increasing of CFRP layers, and the deflection decreased with the increasing of CFRP layers. As shown from **Figures 13-15**, the cracks appeared early in beams with low strengthening. Finaly, it concluded that the presence of FRP has a greater effect on beam capacity and the CFRP layer and thickness play an important issue for failure load of strengthened beams compared with control beam.

5. Conclusions

With the proposed finite element model of RC concrete beam strengthened with CFRP, some conclusions are drawn as follows:

1) The RC beams with flexure strengthened with three layers FRP sheets displayed more load capacity of 60%, 40%, and 30% for one layer, two layers, and three layers, respectively. Also, the cracks generation can be controlled by increasing FRP thickness.

2) All the strengthened beams displayed higher capacities than the equivalent un-strengthened control beams, this confirmed the potential effectiveness of the CFRP sheet applications.

3) Increasing the amount of CFRP strips does not necessarily result in a proportional increase in the flexural capacity of the RC member especially if delamination of CFRP strips controls the failure.

4) The crack mode changed from the large diagonal crack shown by control specimen, which has reinforced with steel, to multiple diagonal cracks covering 97.5% of the length of the specimens reinforced with CFRP.

5) The proposed FE model by using ANSYS can be used as an alternative to experimental work for calculations of first crack, crack width, final load, and mode of failure for beams strengthened with FRP sheets.

Conflicts of Interest

The authors declare no conflicts of interest regarding the publication of this paper.

References

[1] Liu, Y., Zhang, W., Jiang, C., Wu, F., Qiu, J., Wang, R., *et al.* (2025) Flexural Behavior of Reinforced Concrete Beams Subjected to Natural Corrosion in Marine Environment. *Engineering Structures*, **334**, Article ID: 120248. https://doi.org/10.1016/j.engstruct.2025.120248

[2] Ahmed, F.B., Biswas, R.K., Sen, D. and Tasnim, S. (2024) Flexural and Shear Strengthening of Reinforced-Concrete Beams with Ultra-High-Performance Concrete (UHPC). *Construction Materials*, **4**, 468-492. https://doi.org/10.3390/constrmater4020025

[3] Osman, B.H., Wu, E., Ji, B. and Abdulhameed, S.S. (2017) Repair of Pre-Cracked Reinforced Concrete (RC) Beams with Openings Strengthened Using FRP Sheets under Sustained Load. *International Journal of Concrete Structures and Materials*, **11**, 171-183. https://doi.org/10.1007/s40069-016-0182-3

[4] ACI (2005) Building Code Requirements for Structural Concrete "ACI 318-05" and

Commentary (ACI 318-05).

[5] ACI Committee 440 (2000) Guide for the Design and Construction of Externally Bonded FRP System for Strengthening Concrete Structures. ACI Committee 440-F Draft Document, American Concrete Institute.

[6] Teng, J.G., Chen, J.F. and Smith, S.T. (2002) Strengthening of Reinforced Concrete Beams with Externally Bonded Fiber-Reinforced Polymer Composites. *Journal of Structural Engineering*, **128**, 811-823.

[7] Bakht, B. and Jaeger, L.G. (1991) Strengthening of Concrete Structures Using FRP Composites. *Concrete International*, **13**, 34-41.

[8] Benzaamia, A., Ghrici, M., Rebouh, R., Zygouris, N. and Asteris, P.G. (2024) Predicting the Shear Strength of Rectangular RC Beams Strengthened with Externally-Bonded FRP Composites Using Constrained Monotonic Neural Networks. *Engineering Structures*, **313**, Article ID: 118192. https://doi.org/10.1016/j.engstruct.2024.118192

[9] Osman, B.H. (2024) Experimental Study on the Behavior of Pre-Loaded Reinforced Concrete (RC) Deep Beams with Openings Strengthened with FRP Sheets. *World Journal of Engineering*, **22**, 148-159. https://doi.org/10.1108/wje-08-2023-0307

[10] Ozturk, M., Sengun, K. and Arslan, G. (2023) CFRP Contribution to Load-Carrying Capacity of Retrofitted Geopolymer Concrete Beams. *Structures*, **48**, 1391-1402. https://doi.org/10.1016/j.istruc.2023.01.028

[11] Sengun, K. and Arslan, G. (2022) Parameters Affecting the Behaviour of RC Beams Strengthened in Shear and Flexure with Various FRP Systems. *Structures*, **40**, 202-212. https://doi.org/10.1016/j.istruc.2022.04.024

[12] Osman, B.H., Wu, E., Ji, B. and Abdulhameed, S.S. (2017) Shear Behavior of Reinforced Concrete (RC) Beams with Circular Web Openings without Additional Shear Reinforcement. *KSCE Journal of Civil Engineering*, **21**, 296-306. https://doi.org/10.1007/s12205-016-0387-7

[13] Mansur, M.A. and Alwis, W.A.M. (1984) Reinforced Fibre Concrete Deep Beams with Web Openings. *International Journal of Cement Composites and Lightweight Concrete*, **6**, 263-271. https://doi.org/10.1016/0262-5075(84)90021-6

[14] Shanmugam, N.E. and Swaddiwudhipong, S. (1988) Strength of Fibre Reinforced Concrete Deep Beams Containing Openings. *International Journal of Cement Composites and Lightweight Concrete*, **10**, 53-60. https://doi.org/10.1016/0262-5075(88)90022-x

[15] Singh, S.B. (2013) Shear Response and Design of RC Beams Strengthened Using CFRP Laminates. *International Journal of Advanced Structural Engineering*, **5**, Article No. 16. https://doi.org/10.1186/2008-6695-5-16

[16] Nor, N.M., Boestamam, M.A. and Yusof, M.A. (2013) Carbon Fiber Reinforced Polymer (CFRP) as Reinforcement for Concrete Beam. *International Journal of Emerging Technology and Advanced Engineering*, **3**.

[17] Dirar, S., Sogut, K., Caro, M., Rahman, R., Theofanous, M. and Faramarzi, A. (2025) Effect of Shear Span-to-Effective Depth Ratio and FRP Material Type on the Behaviour of RC T-Beams Strengthened in Shear with Embedded FRP Bars. *Engineering Structures*, **332**, Article ID: 120105. https://doi.org/10.1016/j.engstruct.2025.120105

[18] Alsayer, R.B., Solikin, M., Osman, B.H. and Harnaeni, S.R. (2024) Shear Strengthening of Pre-Damaged Reinforced Concrete (RC) Beams Using FRP Sheets.

[19] Osman, B.H., Wu, E., Ji, B. and Abdelgader, A.M. (2016) A State of the Art Review on Reinforced Concrete Beams with Openings Retrofitted with FRP. *International*

Journal of Advanced Structural Engineering, **8**, 253-267. https://doi.org/10.1007/s40091-016-0128-7

[20] Ferreira, D., Oller, E., Marí, A. and Bairán, J. (2013) Numerical Analysis of Shear Critical RC Beams Strengthened in Shear with FRP Sheets. *Journal of Composites for Construction*, **17**. https://doi.org/10.1061/(asce)cc.1943-5614.0000434

[21] Ganganagoudar, A., Mondal, T.G. and Suriya Prakash, S. (2016) Analytical and Finite Element Studies on Behavior of FRP Strengthened RC Beams under Torsion. *Composite Structures*, **153**, 876-885. https://doi.org/10.1016/j.compstruct.2016.07.014

[22] Osman, B.H., Wu, E., Bohai, J. and Abdallah, M. (2017) Repair Technique of Pre-Cracked Reinforced Concrete (RC) Beams with Transverse Openings Strengthened with Steel Plate under Sustained Load. *Journal of Adhesion Science and Technology*, **31**, 2360-2379. https://doi.org/10.1080/01694243.2017.1301073

[23] Valipour, H.R. and Foster, S. (2013) A Mechanistic 1D Finite Element Model for Nonlinear Analysis of FRP-Strengthened Reinforced Concrete Beams. *Advances in Structural Engineering*, **16**, 1989-2004. https://doi.org/10.1260/1369-4332.16.12.1989

[24] Kachlakev, D., Miller, T.R., Yim, S., Chansawat, K. and Potisuk, T. (2001) Finite Element Modeling of Concrete Structures Strengthened with FRP Laminates (No. FHWA-OR-RD-01-17). Oregon. Dept. of Transportation. Research Section.

[25] ANSYS (2004) User's Manual Version 14.5. Swanson Analysis System Inc. (SASI).